Journal of Nepal Chemical Society January 2025, Vol. 45, No. 1, 76-85
DOI: https://doi.org/10.3126/jncs.v45i1.74389
RESEARCH ARTICLE

Synthesis and Characterization of Ferric Oxide-Graphite-Activated Carbon Composites

Mandira Pradhananga Adhikari[1*], Nabin Humagain[1], Biplab Budhathoki[1*]
[1]*Central Department of Chemistry, Tribhuvan University, Kirtipur Kathmandu, Nepal*
[*]*Corresponding E-mail: mandira43@hotmail.com*

(Received: December 8, 2024; revised: December 30, 2024; accepted: January 7, 2025)

Abstract

Activated carbon-based composite electrodes have been widely utilized to enhance the specific capacitance of electrodes. In this study, the effect of the amount of activated carbon on Fe_2O_3-graphite (FGs) was investigated. Fe_2O_3 nanoparticles incorporated with graphite were synthesized using a co-precipitation method. The composites were characterized using X-ray diffraction (XRD), Fourier-transform infrared spectroscopy (FTIR), and UV-Vis spectrophotometry. The FTIR spectra revealed sharp peaks, indicating the successful incorporation of graphite into all four Fe_2O_3 nanoparticle samples in their pure state after calcination. XRD analysis showed that the Fe_2O_3/graphite nano-powders had uniform particle sizes when calcined at 400 °C, with an average crystallite size of approximately 30 nm. The Fe_2O_3-graphite-activated carbon composite prepared with varying amounts of activated carbons (FG-0.25, FG-0.33, FG-0.5, and FG-1.0), was analyzed for its electrochemical performance via cyclic voltammetry (CV). The FG-1.0 composite, with a higher activated carbon content, exhibited a remarkably high capacitance of 1372 F g^{-1}. This significant improvement could be attributed to the dual role of activated carbon as a highly conductive support material and as a provider of an enlarged surface area, which enhances charge transfer efficiency. These findings suggest the potential of Fe_2O_3-graphite-activated carbon composites for large-scale power generation applications.

Keywords: *Activated carbon; Carbon composite; Ferric oxide; Graphite; Supercapacitor*

Introduction

Supercapacitors act as high-power electrochemical energy storage devices and have many applications in the field of electronic, medical, and electrical devices. With the growing demand for high-power, high-reliability, and safe energy storage equipment, the research related to supercapacitors has continued to increase significantly [1,2]. Despite tremendous development in capacitors from the pseudocapacitor to hybrid capacitors, the novel synthesis of effective electrodes needs further research based on the charge storage mechanism. The ideal electrode requirement for Electrochemical Double Layer Capacitors (EDLCs) involves high surface area, porosity, mechanical strength, toughness, electrical conductivity, stability, and enhanced electron transfer [2, 3]. Typically, carbon-based materials are the most widely used materials for EDLC electrodes. Carbon-based anode materials like activated carbon, graphite, and graphene form ideal anode materials as they fulfil most of the above requirements [4-12]. Graphite is an allotrope of carbon with good mechanical strength, electrical conductivity, good availability, and high inertness and is an excellent material for use in supercapacitors

[13-15]. Graphite powder mixed as a binder-free additive to activated carbon material was found to have superior electrochemical properties, where the presence of graphite influenced the microstructure and porosity of the material [16]. Likewise, activated carbon (AC) is a carbon material with a large specific surface area, abundant pores, and a simple preparation process, making it the earliest and most widely used carbon electrode material for supercapacitor electrodes [6, 17-20]. The electric double-layer capacitance of activated carbon is limited to 50 F g^{-1} to 120 F g^{-1} in organic electrolytes, and to 200 F g^{-1} in aqueous electrolytes [21, 22] which causes a lower energy density in carbon-based EDLCs [23].

Composite materials consisting of AC, and transition metal oxides have better capacitive performance due to increased surface area compared to bare transition metal or carbon material [20, 22, 24-30]. Among the metal oxides, Fe_2O_3 is a good candidate due to its high pseudocapacitance [24, 31-33]. Fe_2O_3 was grown on AC cloth which achieved a specific capacitance of 295.56 mA h g^{-1} [22]. A Fe_2O_3-activated carbon composite prepared via the solvothermal method achieved the highest supercapacitance of 240 F g^{-1} [20]. Studies regarding the supercapacitance of graphite electrodes deposited with Fe_2O_3 mixed with ACs are lacking. In addition, the effect of adding AC externally to the Fe2O3-graphite composite and the effect of amounts of AC on the electrochemical performance have not been addressed sufficiently. This study incorporated the synthesis of Fe_2O_3-graphite powder by the coprecipitation method on to which activated carbon was added externally and then characterised by different instrumental techniques. The enhancement of specific capacitance with increasing amounts of ACs was observed and found that the addition of AC was found to be beneficial in improving the supercapacitance of the material

Materials and Methods

Materials

Commercial graphite powder (SD fine-chem Limited, purity ≈ 99.5%), $FeCl_3$ (96% pure, Fisher Scientific), H_2SO_4 (98% pure, Merck), HNO_3 (69%, Merck), NH_4OH (25%, Fisher Scientific), activated carbon (99% pure, Merck) were used. All the chemicals were of analytical grade and used without further purification.

Preparation of Fe_2O_3-graphite composite (FG)

The oxidative surface modification in the case of commercial graphite powder was obtained by reflux boiling of the graphite powder with 1:1 HNO_3 in a 1:10 w/w ratio for 1 hour. After boiling, the mixture was cooled and filtered and then the residue was washed with distilled water till acid-free as confirmed by the litmus test of the filtrate. The graphite so obtained was then dried at 110 °C for an hour in a hot-air over. Finally, the oxidised graphite powder was obtained [34].

Fe_2O_3-graphite nanocomposites were prepared using the co-precipitation method [35]. 1.0, 0.8, 0.6 and 0.4 g of oxidised graphite were taken in a 250 mL beaker and 8, 12, 16 and 20 mL of 0.6 mol L^{-1} $FeCl_3$ were added to each beaker with continuous stirring followed by 100 mL of deoxygenated distilled water to prepare Fe_2O_3-graphite nanocomposites (FG-1, FG-2, FG-3, and FG-4). 2 mol L^{-1} of NH_4OH was added dropwise to maintain a pH value of 11. The resulting mixture was stirred at 80 °C for 3 hours. The precipitate was collected by centrifuging the mixture at 4000 rpm, and then washed with distilled water until neutral. The residue was dried at 100 ℃ for an hour and calcined at 400 ℃ for 1 hour in a muffle furnace.

Incorporation of activated carbon into FG composite

2 g of activated carbon (AC) was taken in a round bottom flask to which 200 mL of 2 N HNO_3 was added and refluxed for 2 hours at 100 ℃. The product was filtered and the residue

was washed with deionized water until the filtrate became neutral to litmus. The residue was dried overnight in a drying oven at 60 ℃ and stored in a desiccator.

The oxidised AC was incorporated into the FG composites, by adding AC to the composite by simple mechanical agitation. Based on the analytical result, the Fe_2O_3 -graphite composite (FG-3) was selected as the best composite for the preparation of the Fe_2O_3-graphite-AC composites. By varying the amounts of Fe_2O_3 nanocomposite (FG-3) and AC as shown in **Table 1**, a series of mixtures containing 1:1, 1:0.5, 1:0.33, and 1:0.25 Fe_2O_3-graphite-AC composites by weight were obtained. The composites were sonicated during the preparation of active material and the preparation of the working electrode for proper mixing and better adherence.

Table 1: Table showing the addition of activated carbon to the FG composites

Composites	FG composite (mg)	Activated carbon (mg)	FG:AC
FG-0	40	0	1:0
FG-0.25	160	40	1:0.25
FG-0.33	120	40	1:0.33
FG-0.5	80	40	1:0.5
FG-1.0	40	40	1:1.0

Characterization of Fe_2O_3-graphite composites

The morphology and chemical composition of the prepared composites were studied using FTIR, XRD, and UV-Vis spectroscopy. The FTIR of the composites were collected using IRPrestige-21 FTIR Spectrometer in the range of 4000 cm−1 to 400 cm^{-1}. The XRD patterns of the synthesized composites were recorded using a Bruker Diffractometer (CuKα λ = 0.154 06 nm) in the range of 20° to 90°. The average crystallite size of Fe_2O_3 was calculated using Scherrer's equation.

$$d = \frac{k\alpha}{\beta cos\theta}$$

where, d = Cystallite size (nm), k = Dimensionless shape factor, α = Wavelength of the X-Ray used (nm), β = Full width at half maximum (FWHM), and θ = Bragg's angle

The UV-Vis spectra of the composites were collected using a Specord 200 Plus Analytik Jena double-beam spectrophotometer.

Electrochemical characterization

For the preparation of the working electrodes, the active material (composite), polyvinylidene fluoride (PVDF) binder, and carbon black were mixed in an 8:1:1 mass ratio. After adding 20 µL of N -Methyl-2-pyrrolidone (NMP), the mixture was slurred, sonicated for 5 minutes, and coated onto 0.5 cm × 0.4 cm nickel foam. The foam was then dried in an electric oven at 60 ℃ for 12 hours. Cyclic voltammograms were obtained on a potentiostat/galvanostat-HA-I5I (HOKUTO DENKO, Japan) by using a three-electrode system. The prepared electrodes were used as the working electrode, platinum wire as the counter electrode, and standard calomel electrode as the reference electrode. 0.5 mol L−1 H2SO4 solution was used as the electrolyte. The cyclic performance of the electrodes was evaluated within a potential window of −0.1 V to 0.8 V.

The specific capacitance was calculated as

$$\text{Specific capacitance} = \frac{\text{Voltammetric Charge}}{\text{Potential window}\times\text{Mass}}$$

The voltammetric charge was calculated from the sum of the anodic and cathodic voltammetric charges which is given by the integral area of the CV curve/scan rate.

$$\text{Voltammetric charge} = \frac{\int i\,(E)dE}{2(E_2 - E_1)mv}$$

where, i(E) = Instantaneous current, $E_2 - E_1$ = Width of potential window, m = Mass deposited, v = Scan rate

Results and Discussion

Morphology and chemical composition of the composite

Fig. 1 shows the XRD pattern of Fe_2O_3 particles before and after calcination. The importance of calcination is visible as two intense peaks were observed at around 26° and 35°. The intense peaks at 35° suggest the formation of Fe_2O_3 nanoparticles after calcination. The XRD of calcined Fe_2O_3 exhibited peaks corresponding to the (012), (104), (110), (113), (024), (116), (018), (214), and (300) confirming the formation of α-Fe_2O_3 particles with a rhombohedral geometry [31]. The average crystallite size of the Fe_2O_3 particles thus prepared was estimated from the full width at half maximum (FWHM) of the most intense peak to be about 30 nm.

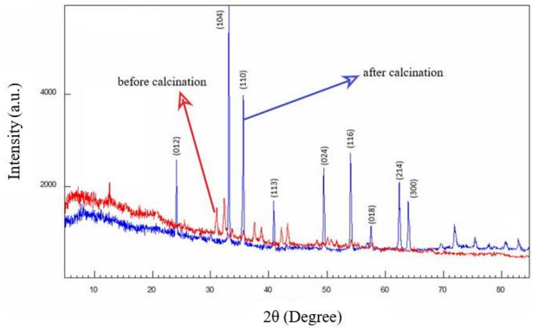

Fig. 1: XRD of Fe_2O_3 before and after calcination.

Fig. 2 shows the XRD patterns of different FG composites. The XRD patterns of the FG-composites show peaks at 2θ = 24, 26.6, 35, 37, 42, 50, 57, 65, and 67 degrees corresponding to the (012), (002) (104), (110), (113), (024), (116), (214), and (216) planes respectively corresponding to rhombohedral geometry of Fe_2O_3 data (JCPDS card no. 01-073-2234) and hexagonal graphite (JCPDS card no. 00-025-0284). These peaks indicate the crystalline nature of the composite. The plane (002) at 2θ = 26.6 is due to the incorporation of graphite in an iron nanoparticle. The presence of two broader peaks around 2θ = 26 and 35, where 2θ = 26 is of graphite while another peak at 35 suggests the formation of Fe_2O_3/graphite composite in all prepared F-G composites having varying concentrations [36]. The broader peak of graphite at 2θ = 26.6 is predominant in the XRD pattern of composite FG-3 in comparison to other composites. It suggests that the incorporation of graphite is in good percentage in this composite. The composite's average crystallite size of the Fe_2O_3 particles formed is approximately 30 nm.

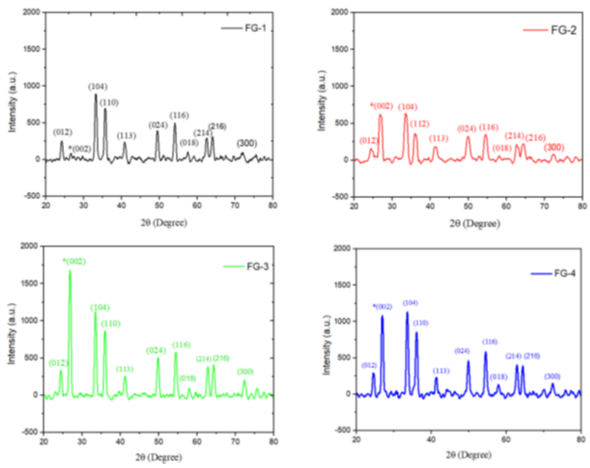

Fig. 2: XRD patterns of FG composites.

The FTIR spectra of different composites are shown in **Fig. 3**. The FTIR spectra of different composites are identical with moderately intense band at 437 cm^{-1}, 1033 cm^{-1}, and 2966 cm^{-1}. The observed peaks in all the samples were almost similar which indicated that the chemical bonding natures of all the samples were almost similar. The strong band below 700 cm^{-1} is assigned to the Fe–O stretching. The band corresponding to the Fe–O stretching mode of Fe_2O_3 is seen at 516 cm−1 [32]. The broad absorption band centered at 2972.2 cm^{-1} and the peak at 2328 cm^{-1} is due to the stretching and bending vibrations of the hydroxyl groups and/or water molecules, respectively [38]. The absorption peaks at around 1627 cm^{-1} and 1454 cm^{-1} are due to asymmetric and symmetric bending vibration of C=O. The observed peaks indicate the presence of hydroxyl groups in addition to a small amount of absorbed water on the same surface of the product as the products were prepared in the aqueous solution. In addition, there is a peak at 1437 cm^{-1} assigned to the deformation of CH_3 [39]. A broader peak is observed at 3398 cm^{-1} in the spectrum of the F-G composite which confirms the doping of graphite in iron particles [40]. The broad band around 3680 cm−1 allocated to the N–H stretching mode is probably due to the impurities present in NH_4OH. The peak corresponding to N–H stretching at 3680 cm^{-1} is broadened and less intense due to the simultaneous occurrence of another new vibrational mode after graphite-doping.

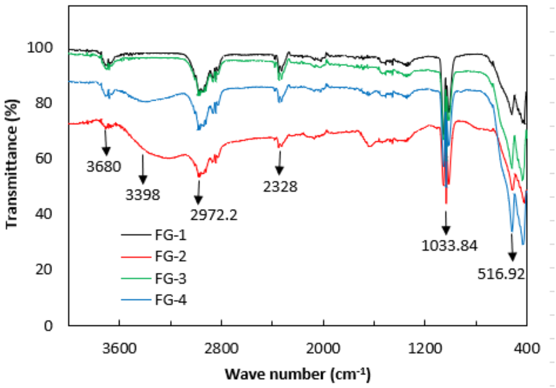

Fig. 3: FTIR spectra of FG composites.

UV-Vis spectra of the FG composites show the absorption spectra in the UV-Vis range of hematite synthesized with different concentrations of Fe_2O_3-graphite show that all absorption curves exhibit a broad absorption peak in the range of 400-600 nm wavelength **(Fig. 4)** [41]. The peak suggested the incorporation of graphite in hematite nanocomposite [37]. Out of all these four F-G composites, the spectrum of FG-2 has more enhancement in absorbance peak compared to other F-G composites most likely from better surface modification and better calcination of the sample. Similarly, FG-3 showed a slightly enhanced peak at around 560 nm which is a good range for the successful incorporation of carbon material in the hematite particles being in good agreement with the results mentioned in earlier work [42]. The results suggested that the sample FG-3 has a better size enhancement with a better % of carbon among all other Fe_2O_3-graphite composites.

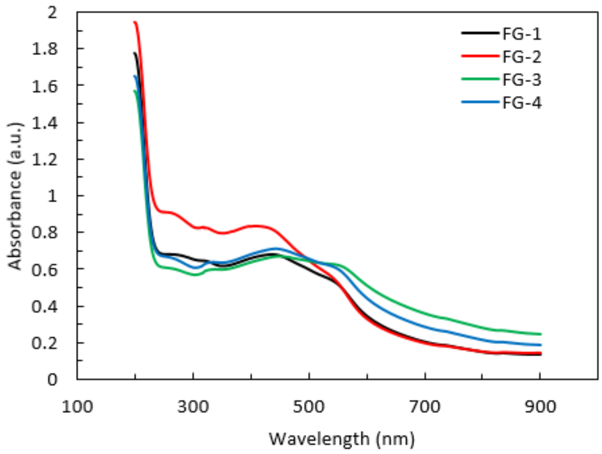

Fig. 4: UV-Vis spectra of FG composites.

Electrochemical characterisation of Fe2O3-graphite-AC composites

Electrochemical measurements were carried out to test the supercapacitance performance of the prepared composite electrodes. Cyclic voltammograms (CVs) of the composites prepared with different weight % of activated carbon in the three-electrode system were recorded at the sweep rate of 20 mV s^{-1}. The fixed operating potential range of −1 V to 0.8 V versus standard calomel electrode (SCE) in 1.0 M H_2SO_4 electrolyte was used. CVs of the composites show oxidation and reduction peaks due to the faradic charge transfer process in the electrode materials, as shown in **Fig. 5**. The specific capacitances of the various composites are shown in Table 2

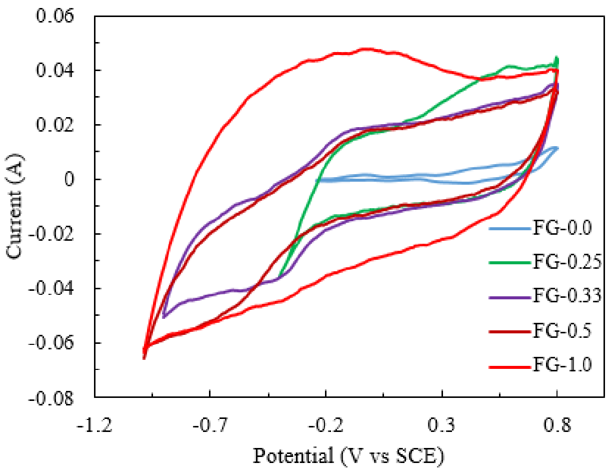

Fig. 5: CV of the FG activated carbon composites.

Table 2: Table showing the specific capacitance of various composites

Composite	Specific capacitance (F g^{-1})
FG-0	35.0
FG-0.25	109.13
FG-0.33	338.21
FG-0.5	398.04
FG-1.0	1372.60

All discharge curves of the voltammogram show a linear behaviour in the voltage range of −1.0 V to 0.8 V in 1M H_2SO_4. Pure Fe_2O_3-graphite (FG-0) delivers an initial specific capacitance of 35.0 F g^{-1}. It is because there may be only pure Fe_2O_3 incorporated with no graphite which makes a composite having no oxidation and reduction cycle [43]. Also, there are no traces of activated carbon involved which can improve the specific capacitance. But when 40 mg of activated carbon was mixed with pure Fe_2O_3-graphite, the specific capacitance of composite material increased significantly. The value of specific capacitance was found maximum at 1372.60 F g^{-1} for the FG-1.0. The composite at a 1:1 ratio of Fe_2O_3-graphite to AC was remarkably higher than those at a lower ratio of Activated carbon supplies. The specific capacitance of FG-0.33 and FG-0.5 are almost similar as a similar amount of activated carbon was loaded during the preparation of these electrodes. The specific capacitance of the FG-AC composite was found to decrease among all the other composites which may be related to the decreasing amount of activated carbon and Ohmic loss arising from material size [44]. This suggests that there is a successful incorporation of activated carbon to a good extent in the FG-1.0 composite which might have contributed to its superior capacitance value. Hence FG-1.0 composites with a 1:1.0 ratio have a good possibility of being a good composite electrode with enhanced electrochemical properties for future use in EDLC, fuel cells, and supercapacitors. Based on the information obtained from the CV analysis and changes in capacitance of different activated carbon incorporated composite electrodes, it is believed that FG-AC electrodes possess a chemical interaction with electrode surface and electrochemical behaviour. Despite the changes in capacitance value due to the incorporation of activated carbon, FG-1.0 composite with a 1:1 ratio is more promising because of high specific capacitance but more investigation should be done regarding the current density and conductivity.

Conclusions

This study introduces a simple and effective method to synthesize cost-effective and efficient supercapacitor electrode materials. Composites of Fe_2O_3-graphite (FG) with varying proportions were synthesized. XRD, FTIR, and UV-Vis spectra were performed to characterize the synthesized composites. XRD spectra suggested the crystalline structure of the Fe_2O_3-graphite composite and the incorporation of Fe_2O_3 nanoparticles in the graphite. The FTIR spectra of Fe_2O_3-graphite also suggested the formation of the Fe–O bond and the introduction of the –OH functional group in the composite. Electrochemical characterization was performed by using cyclic voltammetry. The addition of activated carbon enhanced the specific capacitance and 1:1.0 FG-activated carbon composite was found to have the highest specific capacitance of 1372.60 F g^{-1}. This study was limited in the preparation and characterization of Fe_2O_3-graphite composites and the fabrication of electrode material by adding activated carbon to increase the specific capacitance however, the results suggest a more detailed analysis of composite electrodes using GCD and EIS analysis.

Acknowledgements

Author's Contribution Statement

Mandira P. Adhikari: Conceptualization, Methodology, Writing-review and editing, Supervision, **Biplab Budhathoki:** Experiment, data analysis **Nabin Humagain** Experiment, data analysis, Writing: original manuscript

Conflict of Interest

The authors do not have any conflict of interest throughout this research work.

Data Availability Statement

The data supporting this study's findings are available from the corresponding authors upon reasonable request.

References

1. A. G. Olabi, Q. Abbas, A. A. Makky and M. A. Abdelkareem, Supercapacitors as next generation energy storage devices: Properties and applications, Energy, 2022, 248, 123617, https://doi.org/https://doi.org/10.1016/j.energy.2022.123617
2. W. Raza, F. Ali, N. Raza, et al., Recent advancements in supercapacitor technology, Nano Energy, 2018, 52, 441–473. https://doi.org/10.1016/j.nanoen.2018.08.013
3. B. E. Conway, Electrochemical supercapacitors, Springer US, 1999, https://doi.org/10.1007/9781-4757-3058-6
4. N. Blomquist, T. Wells, B. Andres, J. Backstrom, S. Forsberg and H. Olin, Metal-free supercapacitor with aqueous electrolyte and low-cost carbon materials, Scientific Reports, 2017, 7 (1), 39836. https://doi.org/10.1038/srep39836
5. E. Frackowiak, K. Metenier, V. Bertagna and F. Beguin, Supercapacitor electrodes from multiwalled carbon nanotubes, Applied Physics Letters, 2000, 77 (15), 2421–2423. https://doi.org/10.1063/1.1290146
6. G. Gou, F. Huang, M. Jiang, J. Li and Z. Zhou, Hierarchical porous carbon electrode materials for supercapacitor developed from wheat straw cellulosic foam, Renewable Energy, 2020, 149, 208–216. https://doi.org/10.1016/j.renene.2019.11.150
7. A. Janes, H. Kurig and E. Lust, Characterisation of activated nanoporous carbon for supercapacitor electrode materials, Carbon, 2007, 45 (6), 1226–1233, https://doi.org/10.1016/j.carbon.2007.01.024
8. N. A. Rashidi, Y. H. Chai, I. S. Ismail, M. F. H. Othman and S. Yusup, Biomass as activated carbon precursor and potential in supercapacitor applications, Biomass Conversion and Biorefinery, 2022, https://doi.org/10.1007/s13399-022-02351-1
9. Y. Wang, L. Zhang, H. Hou, et al., Recent progress in carbon-based materials for supercapacitor electrodes: A review, Journal of Materials Science, 2021, 56 (1), 173–200, https://doi.org/10.1007/s10853-020-05157-6
10. Q. Xiao and X. Zhou, The study of multiwalled carbon nanotube deposited with conducting polymer for supercapacitor, Electrochimica Acta, 2003, 48 (5), 575–580,

https://doi.org/10.1016/S0013-4686(02)00727-2

11. H. Yang, S. Kannappan, A. S. Pandian, et al., Graphene supercapacitor with both high power and energy density, Nanotechnology, 2017, 28 (44), 445401, https://doi.org/10.1088/1361-6528/aa8948
12. D. Yu, K. Goh, H. Wang, et al., Scalable synthesis of hierarchically structured carbon nanotube–graphene fibres for capacitive energy storage, Nature Nanotechnology, 2014, 9 (7), 555–562, https://doi.org/10.1038/nano.2014.93
13. G. Ghanashyam and H. K. Jeong, Synthesis of nitrogen-doped plasma treated graphite for supercapacitor applications, Chemical Physics Letters, 2019, 725, 31–37. https://doi.org/https://doi.org/10.1016/j.cplett.2019.04.012
14. H.Y. Li, Y. Yu, L. Liu, L. Liu and Y. Wu, One-step electrochemically expanded graphite foil for flexible all-solid supercapacitor with high rate performance, Electrochimica Acta, 2017, 228, 553–561, https://doi.org/10.1016/j.electacta.2017.01.063
15. Y. Wang, C. Shi, Y. Chen, et al., Self-supported nickel cobalt carbonate hydroxide nanowires encapsulated cathodically expanded graphite paper for supercapacitor electrodes, Electrochimica Acta, 2020, 363, 137236, https://doi.org/10.1016/j.electacta.2020.137236
16. N. S. M. Nor, M. Deraman, M. Suleman, et al., Supercapacitors using binderless activated carbon monoliths electrodes consisting of a graphite additive and pre-carbonized biomass fibers, International Journal of Electrochemical Science, 2017, 12 (3), 2520– 2539. https://doi.org/10.20964/2017.03.48
17. F. Cheng, X. Yang, S. Zhang and W. Lu, Boosting the supercapacitor performances of activated carbon with carbon nanomaterials, Journal of Power Sources, 2020, 450, 227678. https://doi.org/10.1016/j.jpowsour.2019.227678
18. I. I. Gurten Inal and Z. Aktas, Enhancing the performance of activated carbon based scalable supercapacitors by heat treatment, Applied Surface Science, 2020, 514, 145895, https://doi.org/10.1016/j.apsusc.2020.145895
19. M. H. Kim, K. B. Kim, S. M. Park and K. C. Roh, Hierarchically structured activated carbon for ultracapacitors, Scientific Reports, 2016, 6 (1), 21182, https://doi.org/10.1038/srep21182
20. Y. Li, L. Kang, G. Bai, P. Li, et al., Solvothermal synthesis of Fe2O3 loaded activated carbon as electrode materials for high-performance electrochemical capacitors, Electrochimica Acta, 2014, 134, 67–75. https://doi.org/10.1016/j.electacta.2014.04.094
21. E. Frackowiak, Carbon materials for supercapacitor application, Chemical Physics, 2007, 9 (15), 1774–1785. https://doi.org/10.1039/B618139M
22. K. Orisekeh, B. Singh, Y. Olanrewaju, et al., Processing of α-Fe2O3 nanoparticles on activated carbon cloth as binder-free electrode material for supercapacitor energy storage, Journal of Energy Storage, 2021, 33, 102042, https://doi.org/10.1016/j.est.2020.102042
23. H. Shao, Y. C. Wu, Z. Lin, P. L. Taberna and P. Simon, Nanoporous carbon for electrochemical capacitive energy storage, Chemical Society Reviews, 2020, 49 (10), 3005–3039, https://doi.org/10.1039/D0CS00059K
24. B. E. Conway, Transition from “supercapacitor” to “battery” behavior in electrochemical energy storage, Journal of The Electrochemical Society, 1991, 138 (6), 1539. https://doi.org/10.1149/1.2085829
25. K. P. Sharma, A. Arora and S. K. Tripathi, Review of supercapacitors: Materials and devices, Journal of Energy Storage, 2019, 21, 801–825, https://doi.org/10.1016/j.est.2019.01.010

26.H. Shen, Y. Zhang, X. Song, et al., Facile hydrothermal synthesis of actiniaria-shaped α-MnO2/activated carbon and its electrochemical performances of supercapacitor, Journal of Alloys and Compounds, 2019, 770, 926–933, https://doi.org/10.1016/j.jallcom.2018.08.228

27.Y.G. Wang, Z. D. Wang and Y. Y. Xia, An asymmetric supercapacitor using RuO2/TiO2 nanotube com-posite and activated carbon electrodes, Electrochimica Acta, 2005, 50 (28), 5641–5646, https://doi.org/10.1016/j.electacta.2005.03.042

28.J. Xu, F. Liu, X. Peng, et al., Hydrothermal synthesis of NiCo2O4/activated carbon composites for supercapacitor with enhanced cycle performance, ChemistrySelect, 2017, 2 (18), 5189–5195, https://doi.org/10.1002/slct.201700777

29.S. Chen, W. Wang, X. Zhang and X. Wang, High-performance supercapacitor based on graphene/activated carbon hybrid electrodes prepared via dry processing, Batteries 2024, 10, 195. https://doi.org/ 10.3390/batteries10060195

30.D. A. Esteban, S. G. Chamocho, J. C. González, et al., Enhancing electrochemical properies of walnut shell activated carbon with embedded MnO clusters for supercapacitor application, Batteries & Supercaps, 2024, 7, e202400101.doi.org/10.1002/batt.202400101

31.Z. Ma, X., Huang, S. Dou, J. Wu and S. Wang, One-pot synthesis of Fe2O3 nanoparticles on nitrogen-doped graphene as advanced supercapacitor electrode materials, The Journal of Physical Chemistry C, 2014, 118 (31), 17231–17239. https://doi.org/10.1021/jp502226j

32.S. Shivakumara, T. R. Penki and N. Munichandraiah, Synthesis and characterization of porous flowerlike α-Fe2O3 nanostructures for supercapacitor application, ECS Electrochemistry Letters, 2013, 2 (7), A60, https://doi.org/10.1149/2.002307eel

33.R. Lakra, R. Kumar, p. K. Sahoo, S. Kumar and A. Soam, Application of iron oxide in suercapacitor, IntechOpen 2022, DOI: 10.5772/intechopen.105001

34.B. Erable, N. Duteanu, S. M. Senthil Kumar, et al., Nitric acid activation of graphite granules to increase the performance of the non_catalyzed oxygen reduction reaction (ORR) for MFC application, Electrochemistry Communications, 2009, 11(7), 1547-1549. https://doi.org/10.1016/j.elecom.2009.05.057.

35.S. Srivastava and R. R. Pradhananga, S soid Fe2O3-graphite composite electrode for pH measurement, Scientific World, 2014, 12 (12) 14-47.

36.S. Aryal and M. P. Adhikari, Study of composite electrodes of Fe2O3/graphite and MnFe2O4/PANI in microbial fuel cell, Journal of Alpine Chemistry, 2020, https://doi.org/10.6084/m9.figshare.12818795.v2

37.M. Farahmandjou, and F. Soflaee, Synthesis and characterization of α-Fe2O3 nanoparticles by simple co-precipitation method, Physical Chemistry Research, 2015, 3(3), https://doi.org/10.22036/pcr.2015.9193

38.A. Konwar, S. Kalita, J. Kotoky and D. Chowdhury, Chitosan–Iron oxide coated graphene oxide nanocomposite hydrogel: A robust and soft antimicrobial biofilm, ACS Applied Materials & Interfaces, 2016, 8(32), 20625–20634, https://doi.org/10.1021/acsami.6b07510

39.N. K. Rukman, M. Jannatin, G. Supriyanto, M.Z. Fahmi and W. A. W. Ibrahim, GO-Fe3O4 Nanocomposite from coconut shell: Synthesis and characterization, IOP Conference Series: Earth and Environmental Science, 2019, 217, 012008, https://doi.org/10.1088/1755-1315/217/1/012008

40.D. Predoi, A study on iron oxide nanoparticles coated with dextrin obtained by coprecipitation, Digest Journal of Nanomaterials and Biostructures, 2007, 2(1), 169 – 173,

41. A. Lassoued, M. S. Lassoued, F. Karolak, et al., Synthesis, structural, optical, morphological, and magnetic characterization of copper substituted nickel ferrite ($Cu_xNi_{1-x}Fe_2O_4$) through co-precipitation method, Journal of Materials Science: Materials in Electronics, 2017, 28(24), 18480–18488, https://doi.org/10.1007/s10854-017-7795-4
42. A. A. Yaqoob, M. N. M. Ibrahim and S. Rodríguez-Couto, Development and modification of materials to build cost-effective anodes for microbial fuel cells (MFCs): An overview, Biochemical Engineering Journal, 2020, 164, 107779, https://doi.org/10.1016/j.bej.2020.107779
43. M. J. Molaei, A. Ataie, S. Raygan, S. J. Picken and F. D. Tichelaar, Investigation on the effects of milling atmosphere on synthesis of barium ferrite/magnetite nanocomposite. Journal of Superconductivity and Novel Magnetism, 2012, 25(2), 519–524. https://doi.org/10.1007/s10948-011-1322-2
44. E. Darezereshki, F. Bakhtiari, A. B. Vakylabad and Z. Hassani, Single-step synthesis of activated carbon/γ-Fe_2O_3 nano-composite at room temperature, Materials Science in Semiconductor Processing, 2013, 16(1), 221–225. https://doi.org/10.1016/j.mssp.2012.08.007